Core–Shell Structures

DOI: 10.1002/anie.201007077

Gold@Polymer Nanostructures with Tunable Permeability Shells for Selective Catalysis**

Conghui Yuan, Weiang Luo, Lina Zhong, Hujun Deng, Jie Liu, Yiting Xu, and Lizong Dai**

For a functional nanoparticle (NP) encapsulating system, two structural features are especially important: 1) one NP in each capsule (OIC) structure is useful for improving the stability, encapsulating efficiency and physicochemical properties; 2) mesoporous shells not only protect the encapsulated NPs, but can also facilitate the material and energy exchange between the interior and exterior capsule environments. Over the past years, great efforts have been focused on designing and synthesizing nanocomposites possessing one or both of these two features. For example, many noble metal,[1] magnetic,[2] and semiconductor[3] core–shell NPs have unique OIC structure. Especially, the silica-coated metal core–shell system has realized both OIC structure and perfect mesoporous shell.[4–7] Although it is difficult to encapsulate metal or metal oxide with polymer, researchers have obtained many types of metal–polymer or metal oxide–polymer core–shell NPs.[8–13] Commonly, these core–shell systems are prepared using an "inside-out" route. Core NPs are firstly synthesized, and then appropriate methods are used to coat these NPs with predesigned shells. To endow the shell with mesoporous structure, etching methods such as structural difference-based selective etching[4b,c,14,15] and surface-protected etching[5a] have been developed. However, these methods are only suitable for inorganic and inorganic/organic hybrid shells, but are not valid for purely polymeric shells.

Herein, we describe an "outside-in" route to prepare Au@polymer core–shell nanostructures exhibiting both unique OIC structure and controllable mesoporous shells. Au NPs encapsulated in the mesoporous shells exhibit selective catalytic activity. Only hydrophobic molecules can pass through the mesoporous shell and be catalyzed by Au core. The "outside-in" route starts from poly(styrene-*co*-octadecyl,poly(ethylene glycol)-600-butenedioate) (P(St-co-O-B-EG600)) nanospheres, which were synthesized using styrene (St) and octadecyl, poly(ethylene glycol)-600-butenedioate (O-B-EG600)[16] as materials. As illustrated in Figure 1 A, $HAuCl_4$ firstly infiltrates into P(St-*co*-O-B-EG600) nanospheres and etches them into mesoporous structures. Then, ascorbic acid also infiltrates into the mesoporous P(St-*co*-O-B-EG600) nanospheres and reduces $HAuCl_4$. The reduction of $HAuCl_4$ in situ finally results in one Au NP in each capsule. In this route, the formation of mesoporous shells is earlier than that of the cores. So we define it as an "outside-in" route. In this case, $HAuCl_4$ not only acts as etching agent, but also participates in the formation of Au NPs, enabling the synthesis of Au@polymer core–shell nanostructures in one pot.

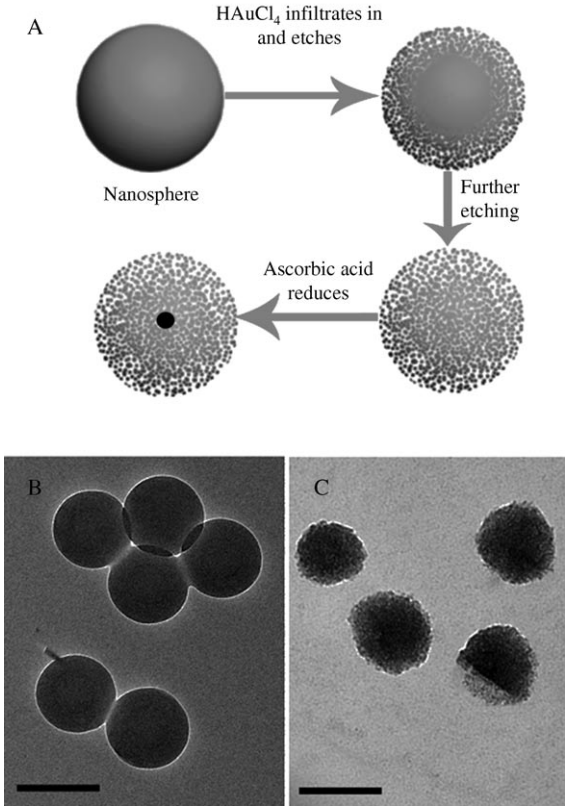

Figure 1. A) Formation of Au@polymer core–shell nanostructures with mesoporous shells. B,C) TEM images of P(St-*co*-O-B-EG600) nanospheres before (B) and after (C) etching by $HAuCl_4$ for 2.0 h. The average diameter of the samples shown in (B) and (C) are (200 ± 5) nm and (170 ± 20) nm, respectively. All scale bars are 200 nm.

[*] Dr. C. Yuan, Dr. W. Luo, L. Zhong, H. Deng, Dr. J. Liu, Prof. Y. Xu, Prof. L. Dai
Department of Materials Science and Engineering
College of Materials, Xiamen University
Xiamen (China)
Fax: (+86) 592-218-3937
E-mail: xyting@xmu.edu.cn
lzdai@xmu.edu.cn

[**] This work was supported by the National Natural Science Foundation of China (50873082, 50903067) and the Scientific and Technical Project of Fujian Province of China (2009J1009, 2010H6021).

Supporting information for this article (^{1}H NMR and UV/Vis spectra, SEM and TEM images, and DLS results of the resultant products.) is available on the WWW under http://dx.doi.org/10.1002/anie.201007077.

During our experimental process, we found that only in the $HAuCl_4$ aqueous solution can the P(St-*co*-O-B-EG600) nanospheres be etched, which reveals that $HAuCl_4$ is the protagonist in this etching system. Figure 1 B,C displays TEM images of P(St-*co*-O-B-EG600) nanospheres before and after etching by $HAuCl_4$ for 2.0 h, respectively. After etching, the nanospheres show a porous structure, and the average diameter becomes slightly smaller (this result was also verified by DLS results shown in Figure S3 in the Supporting Information), indicating that the nanosphere is partially etched. ^{1}H NMR spectroscopy was used to confirm the components of P(St-*co*-O-B-EG600) nanospheres before and after etching (Figure S4 in the Supporting Information). It was found that H proton signals derived from P(O-B-EG600) were weakened significantly after etching. If the etching time is long, the H proton signals of P(O-B-EG600) disappear. These results show that $HAuCl_4$ selectively etches the P(O-B-EG600) component in P(St-*co*-O-B-EG600) nanospheres. We speculate that this etching may be induced by the hydrolysis of the ester group or cleavage of PEG chains in P(O-B-EG600) catalyzed by $HAuCl_4$. However, further investigation still needs to be done.

By simply mixing P(St-*co*-O-B-EG600) nanospheres, $HAuCl_4$, and ascorbic acid in aqueous solution, and allowing the mixture to stand at room temperature for hours, Au@polymer core–shell nanostructures with mesoporous shells are obtained. Figure 2 A–D shows TEM images of Au@polymer nanostructures prepared from reaction times of 2.0, 4.0, 6.0, and 8.0 h, respectively. Clearly, every Au NP with diameter about (15 ± 2) nm is encapsulated in a mesoporous nanosphere (see the magnified image shown in the top-left inset of Figure 2 A), revealing that the Au@polymer nanostructure synthesized using this method has unique mesoporous morphology and efficient encapsulation capability. The bottom-right inset of Figure 2 A displays the electron diffraction pattern of the Au@polymer nanostructure. Clear diffraction disks represent the {220}, {222}, {400}, {420}, and {422} crystal planes of Au. By comparing these four images, it is found that with increasing reaction time, the density of the pore in the polymer shell increases gradually. As the permeability of the polymer shell is decided by the pore density, we consider that the permeability of the polymeric shell in this Au@polymer nanostructure could be easily controlled by the etching time. However, too long an etching time destroys the polymer shell excessively and reduces the encapsulating efficiency (as shown in Figure 2 D). Consequently, to obtain well-defined Au@polymer nanostructures with mesoporous shell, a suitable etching time is important. Careful observation on these four images indicates that the diameter of the Au NP cores does not increase with the increasing reaction time. This result means that the Au NPs have grown fully within the first 2 hours. In the reaction system, $HAuCl_4$ is superfluous. We speculate that the reducing reaction between $HAuCl_4$ and ascorbic acid is complete within the first 2 hours. Thus, prolonged reaction time only induces further etching of polymer shell, but exerts no influence on the diameter of Au NPs. This Au@polymer nanostructure also has tunable diameter. By adjusting the diameter of P(St-*co*-O-B-EG600) nanospheres, Au@polymer nanostructures with diameters ranging from (230 ± 15) nm to (80 ± 15) nm can be easily obtained (see Figure S5 in the Supporting Information).

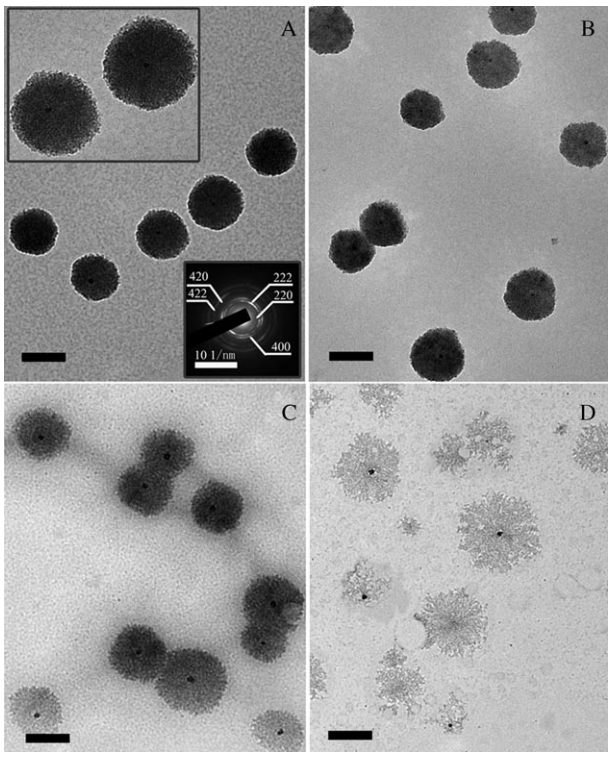

Figure 2. TEM images of Au@polymer nanostructures prepared with various reaction times: A) 2.0 h, B) 4.0 h, C) 6.0 h, D) 8.0 h. The top-left inset of (A) is a magnified TEM image of the Au@polymer nanostructure, and the bottom right inset of (A) is the electron diffraction pattern of the Au@polymer nanostructure. All scale bars are 200 nm.

Restricting NPs in mesoporous shells always allows the free exchange of materials and energy between the exterior environment and the interior cores. Consequently, certain chemical reactions can be carried out on the encapsulated NPs.[5a,13c,17] We found that our mesoporous polymer shell can not only protect the Au NPs, but also endows Au NPs with robust reaction activity. More importantly, Au NPs encapsulated in the mesoporous polymer shells exhibit selective catalytic activity. To verify these useful properties, two experiments were carried out.

Firstly, secondary growth of the Au core in situ was realized through a seed-growing approach using cetyltrimethylammonium bromide (CTAB) to avoid secondary nucleation in solution.[13c,18] Figure 3 A,B gives TEM images of Au@polymer nanostructures obtained from 1.0 and 1.5 h secondary growth time. These two types of Au@polymer nanostructures exhibit (40 ± 5) nm and (60 ± 5) nm diameter Au cores, which are much larger than that of the Au@polymer nanostructures before secondary growth. The increase of the Au core diameter was also proved by the red shift of the absorption peak in UV/Vis spectra (see Figure S6 in the Supporting Information). Thus, it is reasonable to consider that the materials in the environment can transfer into the cores and interact with Au NPs through the mesoporous polymer shells. Moreover, these results also reveal that the

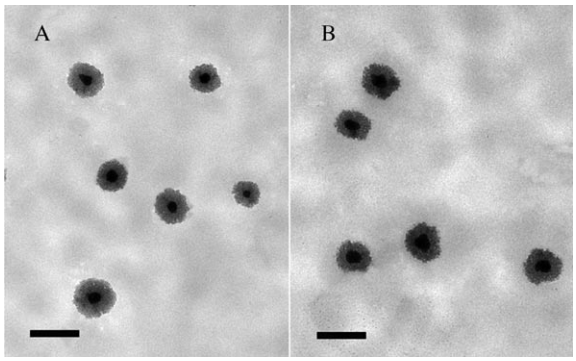

Figure 3. TEM images of Au@polymer nanostructures prepared from 1.0 h (A) and 1.5 h (B) secondary growth times, respectively. The Au@polymer nanostructure with (15 ± 2) nm diameter Au core prepared after 2.0 h reaction time was used as seed. All scale bars are 200 nm.

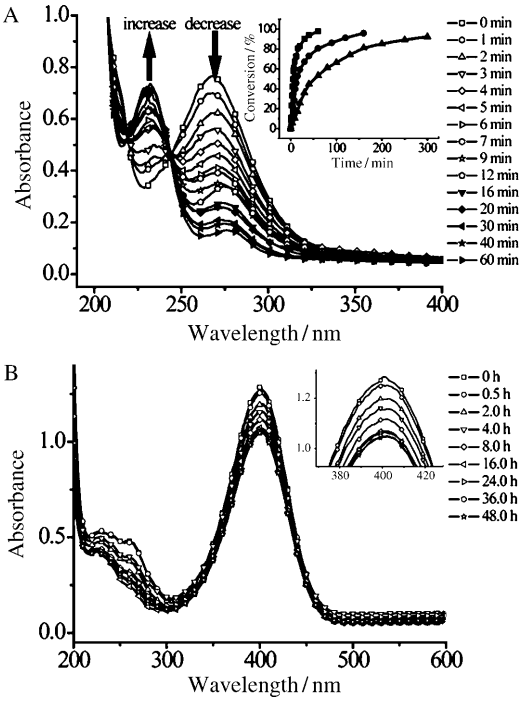

Figure 4. UV/Vis spectra showing the reduction processes of NB (A) and 4-NP (B) with Au@polymer catalyst obtained after 6.0 h reaction time. The inset of (A) shows the conversion of NB using Au@polymer catalyst prepared from 6.0 h (■), 4.0 h (●), and 2.0 h (▲) reaction time, respectively. The inset of (B) is a magnified area of the spectra. All the Au@polymer nanostructures used in the catalyzing experiment have (15 ± 2) nm Au cores. The absorption peak of Au NPs cannot be observed in these UV/Vis spectra, because only a small amount of catalyst was used.

diameter of the Au core could be easily controlled by adjusting the secondary growth time. Comparing Figure 3 with Figure 2 A, it is clear that after the secondary growth, the polymer shells become more hyaline, indicating an evident increase of the pore density in the polymer shell, because the $HAuCl_4$ used for the secondary growth can further etch the polymer shells.

Secondly, we demonstrate that our mesoporous shell can selectively filter hydrophilic molecules, which endows the Au@polymer nanostructures with selective catalytic activity. The Au-catalyzed reductions of hydrophobic nitrobenzene (NB) to aminobenzene (AB) and hydrophilic 4-nitrophenol (4-NP) to 4-aminophenol (4-AP) by $NaBH_4$ were chosen as model reactions. Figure 4 A gives the UV/Vis spectra running after the gradual reduction of NB. It was found that the reduction reaction does not proceed without the Au@polymer nanostructure, regardless of how much $NaBH_4$ is used. However, if a trace amount of the Au@polymer nanostructure is added into the system, the reduction reaction occurs rapidly. The characteristic absorption peak of NB at 275 nm weakens and the characteristic absorption peak of AB at 232 nm increases gradually, which indicates the reduction of NB into AB. This result means that our Au@polymer nanostructure has robust activity for catalyzing the reduction of hydrophobic NB molecules. The inset of Figure 4 A illustrates the influence of the pore density on the catalytic activity of Au@polymer nanostructures. It was found that the Au@polymer nanostructure prepared from a longer reaction time exhibits higher activity for the catalytic reduction of NB. For example, to reach a 90 % conversion, Au@polymer nanostructures prepared from 6.0, 4.0, and 2.0 h reaction time require 30, 120, and 300 min, respectively. As the pore density of the polymer shell is decided by the reaction time, we consider that a higher density of pore results in a higher catalytic activity.

Figure 4 B and its inset shows the UV/Vis spectra tracking the reduction of 4-NP. One can find that the characteristic absorption peak of 4-NP at 400 nm only exhibits a slight decrease and the characteristic absorption peak of 4-AP at around 295 nm does not appear after 2 days. This result means that the Au@polymer nanostructure exhibits almost no catalytic activity for the reduction of 4-NP into 4-AP. Reports have demonstrated that Au NPs have high catalytic activity when using $NaBH_4$ to reduce 4-NP into 4-AP.[19,20] So, it is reasonable to speculate that it is the mesoporous polymer shell barricades the exerting of catalytic activity of the Au core. As the mesoporous polymer shell is prepared by selectively etching the amphiphilic P(O-B-EG600) component, the shell of the Au@polymer nanostructure is mainly composed of hydrophobic PSt. This hydrophobic shell allows hydrophobic molecules to pass through freely, but barricades the transportation of hydrophilic molecules. As a result, hydrophobic NB molecule can pass through the mesoporous polymer shell and be catalyzed by Au NPs, whereas hydrophilic 4-NP cannot pass through the mesoporous polymer shell and be catalyzed by Au NPs. Accordingly, we conclude that the Au@polymer nanostructure can selectively catalyze hydrophobic molecules.

In summary, we have introduced a novel "outside-in" route to encapsulate Au NPs in mesoporous polymer shells. By simply adjusting the reaction time, Au@polymer nanostructures with controllable permeability shells were obtained. As the mesoporous shell allows the materials exchange between inner core and environment, secondary growth of the encapsulated Au NPs can be easily realized. This advantage makes the diameter of the Au core control-

lable. More importantly, the hydrophobic mesoporous shell endows the Au@polymer nanostructure with selective catalytic activity. Only hydrophobic molecules can pass through the hydrophobic shell and be catalyzed by the encapsulated Au NP. We believe that this "outside-in" route may be of interest in encapsulating metal NPs in mesoporous polymer shells, and the selective catalytic activity of this type of Au@polymer nanostructure may prove to be useful in the field of selective catalysis.

Experimental Section

Materials: Maleic anhydride (MA), polyethylene glycol 600 (PEG-600), *p*-toluene sulfonic acid (TSA), and octadecyl alcohol (OA) were purchased from Aldrich. Nitrobenzene (NB), 4-nitrophenol (4-NP), and sodium borohydride ($NaBH_4$) were obtained from Shanghai Chemical Reagent Industry. Styrene (St), cetyltrimethylammonium bromide (CTAB), hydrochloroauric acid ($HAuCl_4$), and ascorbic acid (AA) were analytic grade and supplied by Alfa Aesar. Azoisobutyronitrile (AIBN) was also supplied by Alfa Aesar and recrystallized from methanol before use.

Synthesis of O-B-EG600: O-B-EG600 was synthesized by a two-step esterification reaction using maleic anhydride, octadecyl alcohol, and polyethylene glycol 600 as materials, and *p*-toluene sulfonic acid as catalyst (Scheme S1).[16]

Synthesis of P(St-co-O-B-EG600) nanospheres: Styrene (0.8 mL, 7.0 mmol) and O-B-EG600 (0.5 g, 0.515 mmol) were dispersed in 100 mL (5.56 mol) deionized water. The mixture was stirred for 30 min, and then AIBN (0.04 g, 0.24 mmol) was added in N_2 atmosphere. The reaction mixture was stirred at 72 °C for 6 h. Then, the mixture containing product was evaporated by rotary evaporator to eliminate unreacted styrene and water, and dry P(St-*co*-O-B-EG600) nanospheres were obtained. To obtain P(St-*co*-O-B-EG600) nanospheres with different diameters, 0.4 mL (0.35 mmol), 0.6 mL (5.25 mmol), and 1.2 mL (10.5 mmol), respectively, of styrene was used while keeping the dosage of O-B-EG600 at 0.5 g.

Synthesis of the Au@polymer nanostructures with mesoporous shells: P(St-*co*-O-B-EG600) nanospheres (0.05 g) and CTAB (0.037 g, 0.4 mmol) were dissolved in 22.5 mL of deionized water. Then, $HAuCl_4$ (0.2 mL, 10 mM) and ascorbic acid (AA, 0.5 mL, 0.1M) were added to the mixture at room temperature. The reaction mixture was shaken, and then left undisturbed at room temperature for hours. Au@polymer structure with mesoporous shell was obtained. To control the morphology of the final product, different reaction times, such as 2.0, 4.0, 6.0, and 8.0 h were used.

Confirming the role of $HAuCl_4$ in the etching of P(St-*co*-O-B-EG600) nanospheres: P(St-*co*-O-B-EG600) nanospheres (0.05 g) were dissolved in 22.5 mL of deionized water, and then $HAuCl_4$ (0.2 mL, 10 mM) was added to the mixture at room temperature. The reaction mixture was shaken, and then left undisturbed at room temperature for 2.0 h. The reaction mixture containing the key product was dialyzed in water using a dialytic bag (molecular weight cutoff 3500) to remove unreacted materials and by-products. Transmission electron microscopy (TEM) was used to observe the morphology of P(St-*co*-O-B-EG600) nanospheres before and after etching.

Secondary growth of Au cores: Au@polymer nanostructures with (15 ± 2) nm diameter Au cores prepared from 2.0 h reaction time (0.01 g) and CTAB (0.0093 g, 0.1 mmol) of were dissolved in 5 mL of deionized water. $HAuCl_4$ (0.05 mL, 10 mM) and ascorbic acid (AA, 0.5 mL, 0.1M) were added to the mixture at room temperature. The reaction mixture was shaken, and then left undisturbed at room temperature for hours. The diameter of the Au core was controlled by the secondary growing time.

Catalytic reduction of nitrobenzene (NB) and 4-nitrophenol (4-NP): The reduction reactions of NB and 4-NP by $NaBH_4$ were chosen as model reactions to test the selective catalytic activity of the Au@polymer nanostructure. Aqueous solutions of NB (0.04 mL, 0.01M) and 4-NP (0.04 mL, 0.01M) were added into quartz cuvettes filled with 2.0 mL deionized water under magnetic stirring. Aqueous $NaBH_4$ (0.4 mL, 0.1M) and an aqueous solution of Au@polymer nanostructures (0.1 mL, 0.05 mg mL^{-1}) were added to the two quartz cuvettes. UV/Vis spectra were recorded at regular intervals to monitor the progress of the reaction.

Characterization: ^1H NMR spectra of the products were measured on a Bruker ARX 400 MHz spectrometer for 1000 scans at a relaxation time of 2 s. UV/Vis spectra of the samples in aqueous solutions were measured on a Unico UV/Vis 2802PCS instrument. The particle sizes of the products were characterized by dynamic light scattering (DLS) on a ZetaPALS instrument.

TEM measurements and electron diffraction experiment were performed with a JEM2100 microscope at an acceleration voltage of 200 kV. To prepare the TEM samples, a small drop of Au@polymer structure solution was deposited onto a carbon-coated copper electron microscopy (EM) grid and then dried at room temperature.

SEM images were obtained from a field emission scanning electron microscope (FE-SEM, LEO-1530). Samples were dispersed in deionized water. The mixtures were then dropped on aluminum sheets. After air-drying for 24 h at room temperature, the samples were treated by gold sputtering.

Received: November 10, 2010
Revised: December 26, 2010
Published online: March 8, 2011

Keywords: chemoselectivity · gold · heterogeneous catalysis · mesoporous materials · nanoparticles

[1] a) Y. W. Cao, R. C. Jin, C. A. Mirkin, *J. Am. Chem. Soc.* **2001**, *123*, 7961 – 7962; b) F. R. Fan, D. Y. Liu, Y. F. Wu, S. Duan, Z. X. Xie, Z. Y. Jiang, Z. Q. Tian, *J. Am. Chem. Soc.* **2008**, *130*, 6949 – 6951; c) Y. Lu, Y. Zhao, L. Yu, L. Dong, C. Shi, M. J. Hu, Y. J. Xu, L. P. Wen, S. H. Yu, *Adv. Mater.* **2010**, *22*, 1407 – 1411.

[2] a) Y. Deng, D. Qi, C. Deng, X. Zhang, D. Zhao, *J. Am. Chem. Soc.* **2008**, *130*, 28 – 29; b) K. Cheng, S. Peng, C. Xu, S. Sun, *J. Am. Chem. Soc.* **2009**, *131*, 10637 – 10644; c) V. Mazumder, M. Chi, K. L. More, S. Sun, *J. Am. Chem. Soc.* **2010**, *132*, 7848 – 7849.

[3] T. Nann, P. Mulvaney, *Angew. Chem.* **2004**, *116*, 5511 – 5514; *Chem. Int. Ed.* **2004**, *43*, 5393 – 5396.

[4] a) Y. S. Li, J. L. Shi, Z. L. Hua, H. R. Chen, M. L. Ruan, D. S. Yan, *Nano Lett.* **2003**, *3*, 609 – 612; b) Y. Chen, H. Chen, L. Guo, Q. He, F. Chen, J. Zhou, J. Feng, J. Shi, *ACS Nano* **2010**, *4*, 529 – 539; c) Y. Chen, H. Chen, D. Zeng, Y. Tian, F. Chen, J. Feng, J. Shi, *ACS Nano* **2010**, *4*, 529 – 539.

[5] a) Q. Zhang, T. Zhang, J. Ge, Y. Yin, *Nano Lett.* **2008**, *8*, 2867 – 2871; b) Y. Deng, Y. Cai, Z. Sun, J. Liu, C. Liu, L. Wei, W. Li, C. Liu, Y. Wang, D. Zhao, *J. Am. Chem. Soc.* **2010**, *132*, 8466 – 8473.

[6] X. J. Wu, D. Xu, *J. Am. Chem. Soc.* **2009**, *131*, 2774 – 2775.

[7] T. R. Zhang, J. P. Ge, Y. X. Hu, Q. Zhang, S. Aloni, Y. D. Yin, *Angew. Chem.* **2008**, *120*, 5890 – 5895; *Angew. Chem. Int. Ed.* **2008**, *47*, 5806 – 5811.

[8] W. P. Wuelfing, S. M. Gross, D. T. Miles, R. W. Murray, *J. Am. Chem. Soc.* **1998**, *120*, 12696 – 12697.

[9] a) K. J. Watson, J. Zhu, S. T. Nguyen, C. A. Mirkin, *J. Am. Chem. Soc.* **1999**, *121*, 462 – 463; b) D. Gittins, F. Caruso, *J. Phys. Chem. B* **2001**, *105*, 6846 – 6852; c) A. B. Lowe, B. S. Sumerlin, M. S. Donovan, C. L. McCormick, *J. Am. Chem. Soc.* **2002**, *124*, 11562 – 11563.

[10] M.-Q. Zhu, L.-Q. Wang, G. J. Exarhos, A. D. Q. Li, *J. Am. Chem. Soc.* **2004**, *126*, 2656 – 2657.

[11] a) I. Gorelikov, L. M. Field, E. Kumacheva, *J. Am. Chem. Soc.* **2004**, *126*, 15938 – 15939; b) S. Nayak, L. A. Lyon, *Angew. Chem.*

2005, *117*, 7862 – 7886; *Angew. Chem. Int. Ed.* **2005**, *44*, 7686 – 7708; c) Y. Kang, T. A. Taton, *Angew. Chem.* **2005**, *117*, 413 – 416; *Angew. Chem. Int. Ed.* **2005**, *44*, 409 – 416; d) H. Dong, M. Zhu, J. A. Yoon, H. Gao, R. Jin, K. Matyjaszewski, *J. Am. Chem. Soc.* **2008**, *130*, 12852 – 12853.

[12] a) P. J. Roth, P. Theato, *Chem. Mater.* **2008**, *20*, 1614 – 1621; b) S. Abraham, I. Kim, C. A. Batt, *Angew. Chem.* **2007**, *119*, 5822 – 5825; *Angew. Chem. Int. Ed.* **2007**, *46*, 5720 – 5723.

[13] a) R. Álvarez-Puebla, R. Contreras-Cáceres, I. Pastoriza-Santos, J. Pérez-Juste, L. M. Liz-Marzán, *Angew. Chem.* **2009**, *121*, 144 – 149; *Angew. Chem. Int. Ed.* **2009**, *48*, 138 – 143; b) R. Contreras-Cáceres, J. Pacifico, I. Pastoriza-Santos, J. Pérez-Juste, A. Fernández-Barbero, L. M. Liz-Marzán, *Adv. Funct. Mater.* **2009**, *19*, 3070 – 3076; c) R. Contreras-Cáceres, A. Sánchez-Iglesias, M. Karg, I. Pastoriza-Santos, J. Pérez-Juste, J. Acifico, T. Hellweg, A. Fernández-Barbero, L. M. Liz-Marzán, *Adv. Mater.* **2008**, *20*, 1666 – 1670.

[14] S. B. Yoon, K. Sohn, J. Y. Kim, C. H. Shim, J. S. Yu, T. Hyeon, *Adv. Mater.* **2002**, *14*, 19 – 21.

[15] M. Kim, K. Sohn, Y. B. Na, T. Hyeon, *Nano Lett.* **2002**, *2*, 1383 – 1387.

[16] a) C. H. Yuan, Y. T. Xu, Y. M. Deng, J. F. Chen, Y. L. Liu, L. Z. Dai, *Soft Matter* **2009**, *5*, 4642 – 4646; b) C. H. Yuan, Y. T. Xu, Y. F. Liao, S. J. Lin, N. He, L. Z. Dai, *J. Mater. Chem.* **2010**, *20*, 9968 – 9975.

[17] a) Y. Lu, Y. Mei, M. Ballauff, *J. Phys. Chem. B* **2006**, *110*, 3930 – 3937; b) Y. Mei, Y. Lu, F. Polzer, M. Ballauff, *Chem. Mater.* **2007**, *19*, 1062 – 1069; c) M. Schrinner, S. Proch, Y. Mei, R. Kempe, N. Miyajima, M. Ballauff, *Adv. Mater.* **2008**, *20*, 1928 – 1933; d) M. Karg, T. Hellweg, *J. Mater. Chem.* **2009**, *19*, 8714 – 8727.

[18] J. Rodríguez-Fernández, J. Pérez-Juste, F. J. García de Abajo, L. M. Liz-Marzán, *Langmuir* **2006**, *22*, 7007 – 7010.

[19] Y. Lu, Y. Mei, M. Drechsler, M. Ballauff, *Angew. Chem.* **2006**, *118*, 827 – 830; *Angew. Chem. Int. Ed.* **2006**, *45*, 813 – 816.

[20] a) S. Panigrahi, S. Basu, S. Praharaj, S. Pande, S. Jana, A. Pal, S. K. Ghosh, T. Pal, *J. Phys. Chem. C* **2007**, *111*, 4596 – 4605; b) J. Lee, J. C. Park, H. Song, *Adv. Mater.* **2008**, *20*, 1523 – 1528.

